SLAC-PUB-3311
IUHEP-54
April 1984
(I)

RECENT DEVELOPMENTS IN HIGH PRECISION VERTEX CHAMBERS AT SLAC*

DAVID R. RUST
Department of Physics
Indiana University, Bloomington, Indiana 47405
and
Stanford Linear Accelerator Center
Stanford University Stanford, California 94305

ABSTRACT

Three detectors MARK II, MAC, and HRS are using or planning small drift chambers placed as close as possible to the interaction print at PEP. There is also a program of development for a gaseous vertex detector for MARK II at SLC. All these programs are reviewed in this paper.

1. INTRODUCTION

I have grouped two classes of chambers into this one talk. One class has very high resolution ($\sim 20\,\mu m$) and the other has moderately high resolution ($\sim 100\,\mu m$) but is simpler to construct.

I would like to begin by discussing some of the experiences with the MARK II vertex chamber. At the time of the 1982 meeting of this conference it had been installed and had taken data amounting to a few pb^{-1} of integrated luminosity[1] and true measures of its performance were lacking. It has continued to take data up to the present time and by the end of this running period it should have taken about 180 pb^{-1} total integrated luminosity.

The longitudinal sectional view of this chamber is shown in Fig. 1 and the cell structure of the inner band of wires is shown in Fig. 2. For other details refer to Ref. 1. The chamber has operated at atmospheric pressure (50% ethane in argon) for all the data taking. For real conditions of data taking the average spatial resolution is $\sigma = 110\,\mu m$ per layer for hadronic events and somewhat better than that for QED events. Figure 3 shows a good measure of the quality of any vertex chamber

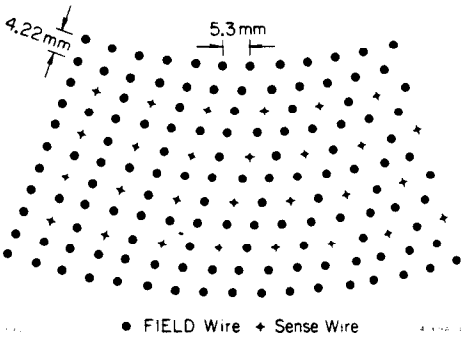

Fig. 2. Arrangement of wires in the MARK II vertex detector. One half of one section of the inner band is shown.

at an $e^+ - e^-$ collider, the distance between tracks of Bhabha events at the interaction point. For hadronic events the position resolution for a track at the interaction point is $\sigma(\mu m) = \sqrt{(95)^2 + (95/p)^2}$ (p in GeV/c). This chamber has proved its usefulness by measuring three important lifetimes: the tau lepton[2], b hadrons[3] and the D^o meson.[4] In each measurement the decay length is less than or much less than 1 mm at the laboratory momentum of the particle. The resolution of the vertex chamber is good enough so that the main contribution to the width of the decay length distribution comes from the width of the beam.

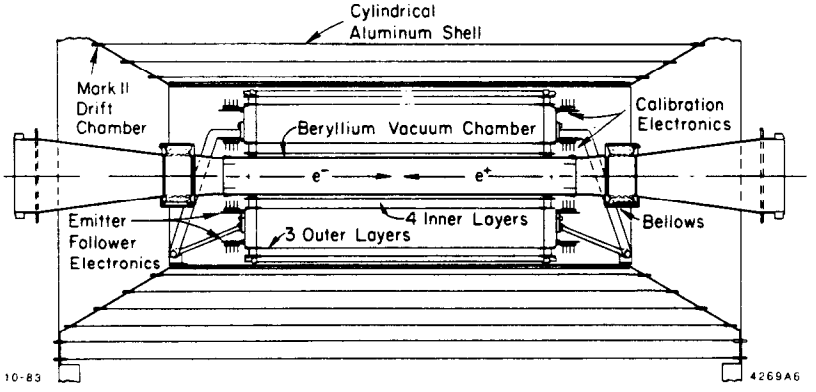

Fig. 1. Cross section of the MARK II vertex detector.

* Work supported by the Department of Energy contracts, DE-AC03-76SF00515 (SLAC) and DOE-AC02-84ER40125 (Indiana).

Invited paper presented at the 3rd International Conference on Instrumentation for colliding Beam Physics, Novosibirsk, U.S.S.R, March 15-21, 1984

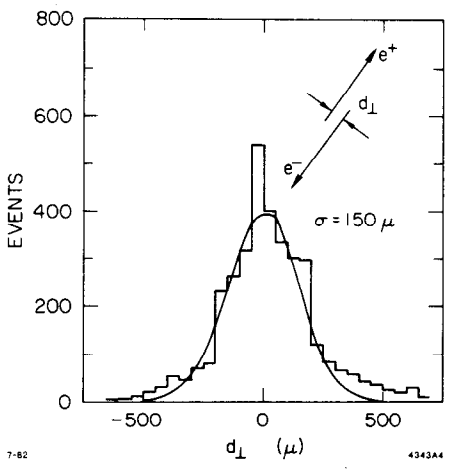

Fig. 3. Distance between tracks in Bhabha events measured at the interaction point.

2. CHAMBERS MADE FROM SMALL THIN TUBES

A chamber of this type is operating at the HRS and others are planned both for MAC and MARK II.

When a small, thin and reliable chamber was needed for the HRS detector to reduce the cosmic ray trigger rate and improve tracking near the interaction point, it was decided to use the tube design. The most attractive feature was that the cells are all isolated from each other so that if a problem such as a broken wire or a discharge point develops in one cell it can be disconnected without affecting the rest of the chamber. This consideration was important because the chamber is inaccessible in its position in the detector. A failure which would disable a significant fraction of the chamber would render it useless for a long period of time and it was therefore important to make fail-safe device.

Drift chambers made from small thin aluminum tubes have used before at e^+e^- storage rings. Some tests were reported by Becker et al.[5] and a working chamber was constructed for MARK J and also for CELLO at PETRA. Experience at SLAC in the use of such tubes was gained at the Crystal Ball detector operating at SPEAR and DORIS although these tubes were only operated as proportional counters.

The innovation which is incorporated into the HRS inner tracking chamber is the use of mylar tubes with an aluminized inner surface instead of solid aluminum tubes. The advantages of the aluminized mylar tubes are that they have smaller average Z and therefore less multiple scattering and that they are not so easily damaged because mylar is tough and resilient.

There were two difficulties to be overcome. One was in manufacturing the tubes from aluminized mylar without scratching the thin aluminum coating. The tube manufacturer[6] succeeded in developing a process to make acceptable tubes without scratches. The aluminized mylar in the form of a strip is wound around a polished rod. The winding is done so there is no overlap of one turn of the strip onto the next and as little space as possible between them. A second layer of clear mylar is then glued over the first so that the joint in the first layer is completely covered and the tube wall is of uniform thickness.

The other difficulty was to make a reliable contact to the inner aluminum coating. A high quality creamy silver loaded epoxy[7] has been used with good success.

An independent effort at the Institute for Nuclear Physics at Novosibirsk has also succeeded in making drift tubes out of aluminized mylar[8]. The tubes are made by a different process but the results are essentially the same.

The tube pattern of the HRS inner tracking chamber is shown in Fig. 4. It was necessary to fit it into the existing detector without removing the beam pipe. There was therefore only room for four layers and it was necessary to split the chamber into two halves which were then assembled around the beam pipe. The longitudinal rigidity was provided only by the tubes themselves but the structure was very strong. The tubes were glued to each other all along their length and a skin of mylar was glued both on the inside and the outside of each double of layer tubes for additional strength. The only volume containing gas was in the tubes themselves. Mounting rings (Fig. 5) were glued to each end of the tube structure to

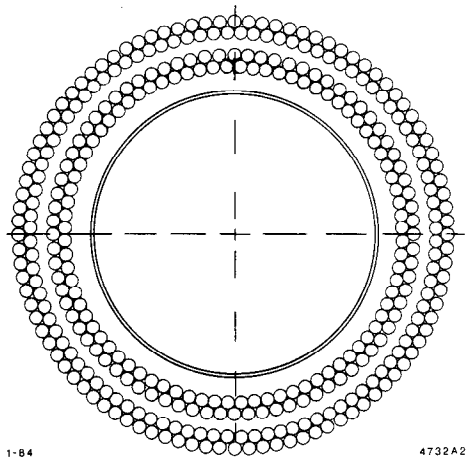

Fig. 4. Cross-section of the HRS inner tracking chamber and the PEP beam pipe.

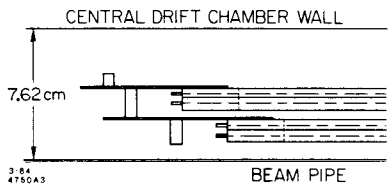

Fig. 5. Sectional diagram of one end of the HRS inner tracking chamber showing the basic construction scheme.

provide a means of coupling layers to each other and also to the mounting brackets.

The tubes must be held straight because they bend easily. Alignment of the tubes to $\pm 100\,\mu m$ during construction was accomplished using precisely machined forms.

The mechanical design including the wire positioning system was quite similar to that used in the Crystal Ball inner tracking chamber. Precisely machined Delrin plugs were glued into each end of each tube using conductive epoxy. At the same time a wire was incorporated into the assembly to provide an electrical path to the inner surface of the tube through the conductive epoxy (Fig. 6). The sense wire was strung through a tubule with a $100\,\mu m$ inner diameter. This tubule nested in a larger tubule which was in turn seated into the Delrin plug. The positioning error was minimized by pulling the sense wire always to the same side of the plug during the crimping operation. The crimp joint was reinforced by an epoxy bead.

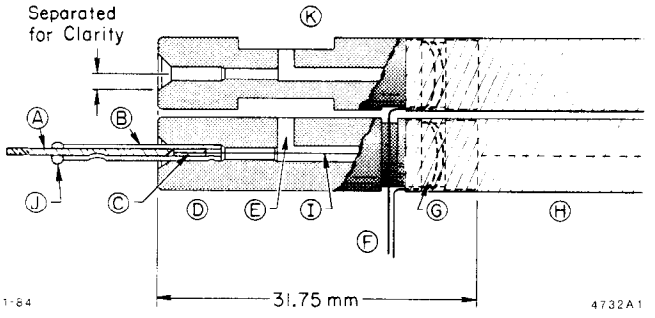

Fig. 6. Detail of the Delrin plug showing the nested wire positioning tubules *B*, *C*; the Delrin plug, D; the gas inlet hole, E; the wires connecting to the inside surface of the tube, F; the wires wrapped around a groove in the Delrin plug, G; the mylar tube, H; the sense wire, I; the expoxy bead, J; the gas channel, K; A is soft brass wire crimped together with the tubule and the sense wire.

Table I lists some physical and mechanical characteristics of the HRS inner tracker. It was installed in September 1983 and has been taking data since December 1983. We now have enough Bhabha events to align and calibrate the chamber and determine its resolution. The double layer tube pattern makes the chamber self-calibrating on high momentum tracks such as in Bhabha scattering. With a gas mixture of 25% ethane in argon and a 1.6 *T* magnetic field the drift distance is a quadratic function of drift time. The tube resolution obtained from the simultaneous measurement of the same tracks in overlapping tubes gives $\sigma = 130\,\mu m$ in agreement with Ref. 5. The resolution at the vertex is a result of using the main drift chamber together with the inner tracker. The Bhabha track separation distribution at the interaction point has $\sigma = 270\,\mu m$. The cosmic ray trigger rate has been reduced to .6 Hz.

TABLE I

Specifications for the HRS inner tracking chamber

	Layer 1	Layer 2	Layer 3	Layer 4
Number of tubes	80	80	96	96
radius (cm)	9.096	9.714	10.915	11.534
active length (cm)	40.6	40.6	45.7	45.7
tube inner diam. (cm)	.691	.691	.691	.691
angular position of wire number 1	.0426	.0033	.0328	.000

Total chamber thickness = .004 R. L.

Largely because of the practical advantages of the tube design two similar detectors are being built now: one for MARK II and one for MAC. The one built for MARK II will function mainly as a trigger chamber as at the HRS and will fit inside the new MARK II central drift chamber. (The former vertex chamber is too big to fit inside the new drift chamber). The one built for MAC is meant to emphasize good resolution for tracking to a vertex and will be pressurized.

The MARK II trigger chamber is being built by W. T. Ford and his group at the University of Colorado and incorporates some evolutionary design changes over the HRS model. The chamber structural element is a rigid foam shell which also encloses the gas volume on the outside. Precision drilled end caps locate the holes in which plugs are inserted to position the tubes and the wires. The tubes as well as the wires are stretched to keep them straight (Fig. 7). (The mylar tubes withstand large forces along their length and also are able to hold a large overpressure.) This chamber is expected to be ready for operation by the end of 1984.

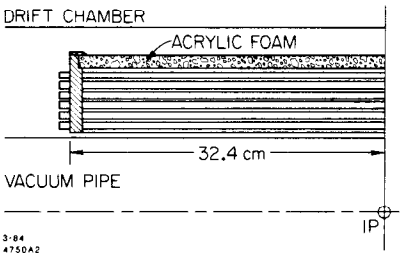

Fig. 7. Sectional drawing showing the basic construction of the MARK II trigger chamber.

The MAC vertex chamber is intended to supplement the present tracking system to improve the capability for measuring *B* and *tau* lifetimes. the goal is to achieve $80\,\mu m$ resolution by running the chamber at 2 atmospheres. This chamber will be constructed as an integral part of a new vacuum pipe which will have an inner diameter of 7.1 cm instead of the usual 15 cm diameter. A new masking scheme has been designed to mask the chamber from synchrotron radiation at this small distance

from the beam. Although there is some experience with operating the main MAC drift chamber with a beam pipe about 7 cm in diameter, there is none with operating a chamber so close to the PEP beam. In this situation with possibly a high radiation environment it was thought that the tube design would be more reliable than one with wire cathodes or with field shaping wires.

The MAC design uses a beryllium inner cylinder to support the tension and precision drilled end plates to position the plugs which hold the tubes and the wires in position. As in the MARK II version the tubes will be stretched to keep them straight. The chamber structure will then be enclosed by a pressure vessel consisting of the beam pipe on the inner diameter, feed-through rings on the ends and an outer covering plate.

Some of the specifications for the MARK II trigger chamber and the MAC vertex chamber are given in Table II.

TABLE II

Some specifications of the MARK II and MAC tube chambers

	MARK II	MAC
Number of layers	6	6
Number of tubes	72, 80, 88,	40, 40, 54,
per layer	96, 104, 112	54, 68, 68
Tube diameter (mm)	7.9	7.1
length (cm)	~60	~60
inner layer radius (cm)	9.1	4.5
outer layer radius (cm)	14.2	8.3
operating pressure (atm)	1	≥ 2

3. STUDIES COMPARING THE TUBE DESIGN WITH THE JET CHAMBER DESIGN

In this paper the term "jet chamber" refers to the general cell structure shown in Figs. 9 and 12. This structure was first used on a large scale in the JADE main tracking chamber[13] which was called the jet chamber because it was used to observe jets of particles.

The MAC group made a study of the expected resolution of the tube type chamber and compared the results to the resolution expected from a jet chamber.[9] They used a program by Va'vra[10] to simulate the complete chain of events from the time a minimum ionizing particle crosses the cell to the time at which the resulting pulse appears at the input of the discriminator. A saturated gas (50% ethane in argon) was assumed. Other characteristics of the two chamber designs are given in Table III.

TABLE III

Specifications of chambers
compared using a Monte Carlo simulation

jet chamber parameters:	
drift length	8.4 to 13.9 mm
cell width	5 mm
sense wire diam.	20 μm
potential wire diam.	100 μm
sense wire potential	0 V
potential wire potential	-1.44 kV
cathode wires potential	-2.56 to -3.69 kV
magnetic field	5.7 kG
tube parameters:	
tube diam.	8 mm
sense wire diam.	20 μm
E field at cathode	.6 kV/cm
magnetic field	5.7 kG

The conclusion was that the two designs were not very different with respect to resolution contributed by geometric and statistical effects. This is illustrated in Fig. 8 where the pulse shape referenced to a fixed time is plotted. It is important in any case to be sensitive to the first electron that arrives if one wants good resolution. Beyond that, however, there are several important considerations. There is clearly no double track resolution capability in a tube operating with one electron sensitivity because electrons from any track continue to

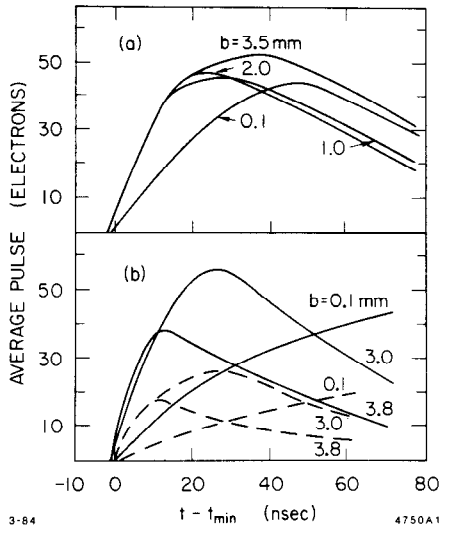

Fig. 8. Pulse shapes generated by a Monte Carlo program for a jet chamber cell (a) and a tube chamber cell (b). The solid lines are for a pressure of 2 atm and the dotted lines for 1 atm. the parameter b is the distance of the track to the sense wire. t_{min} is the time for an electron to drift the distance b.

arrive over the maximum drift time and cover up electrons from any track at larger distance from the wire. The jet chamber design is much better in this respect. The jet chamber also requires many fewer sense wires. The tube chamber, however, provides naturally for ambiguity resolution when constructed as, for example, in Fig. 4 and, as mentioned before, can be made less sensitive to failures.

4. STUDIES WITH MICROJET CHAMBERS

There has been much interest in developing chambers with very high resolution ($\sim 20\,\mu m$) and also good multi track capability for colliding beam detectors. This interest is prompted by the need to measure closely spaced particles in jets at the higher energy machines such as SLC.

About three years ago a small pressurized drift chamber of the jet type was built for fixed target experiment at the SPS.[11] The resolution in a low intensity beam with 4 atmospheres of 25% ethylene in propane was $23\,\mu m$. The length of the wires was about 10 cm.

About one year ago Va'vra[12] reported the results of his tests on a prototype chamber with $\sim 20\,\mu m$ resolution. He tried a number of different gases at pressures up to 6 atmospheres. The physical and electronic arrangement of the components for this test is shown in Fig. 9. The resolution as a function of impact parameter in 10% isobutane in argon at 6 atm is shown in Fig. 10. The double track resolution without pulse shaping and with simple time over threshold discriminators was estimated at $\sim 3/4\,mm$.

Since then some further development work has been carried out by J. Jaros and K. Hayes with the goal of building a vertex chamber for use in the MARK II detector operating at SLC. A practical chamber is needed with resolution $< 30\,\mu m$

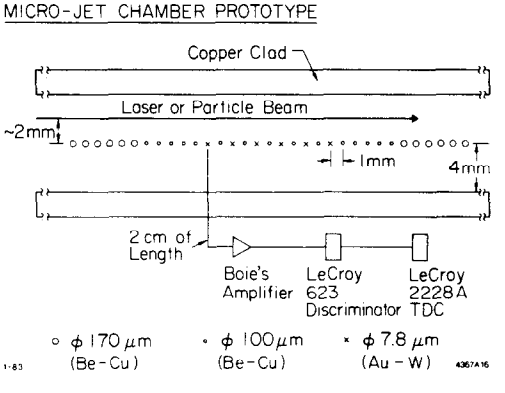

Fig. 9. Arrangement of components for a test of a prototype micro-jet chamber. The sense wires are × and the potential wires are o.

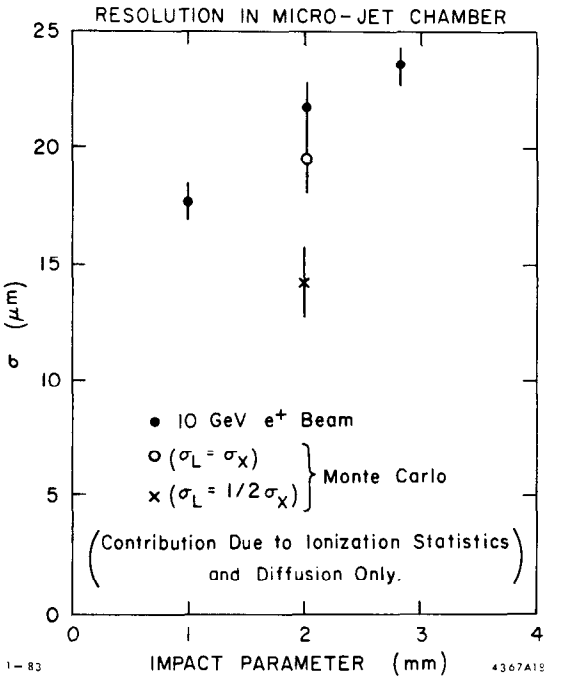

Fig. 10. Resolution of the prototype micro-jet chamber at 6.1 atm 10% iso butane in argon.

and adjacent track separation distance $\sim 250\,\mu m$. Several cell geometries have been considered and studied using basically the same simulation program that Va'vra and the MAC group used.

An important figure of merit for a jet chamber cell is the curvature of the lines of constant drift time in the drift region far from the sense wire. It was found that over $\sim 2/3$ of the width of a cell the lines can be parametrized by $x = -C(y - y_0)^2$ where x is along the drift direction, y is perpendicular both to the sense wire and to x and y_0 is the position of the sense wire. By making C smaller one makes the spread in arrival times of the electrons smaller and one obtains at the same time both better position resolution and better adjacent track separation.

Figure 11 shows the dependence of the resolution in a simple jet chamber (see inset in Fig. 12) on the constant C for various triggering levels in a diffusionless gas with drift velocity $50\,\mu m/ns$. This illustrates the importance of a low triggering level as well as the need for a small value of C. If diffusion is allowed to be non-zero we have the relationship shown in Fig. 12 for drift velocity $= 25\,\mu m/ns$. Both of these curves are for a sense wire spacing of 1 mm and primary ionization of 100 electrons/cm. Clearly a gas with the smallest diffusion constant is needed together with small C and small cell width so that the spread of arrival times at the sense wire is as small as possible.

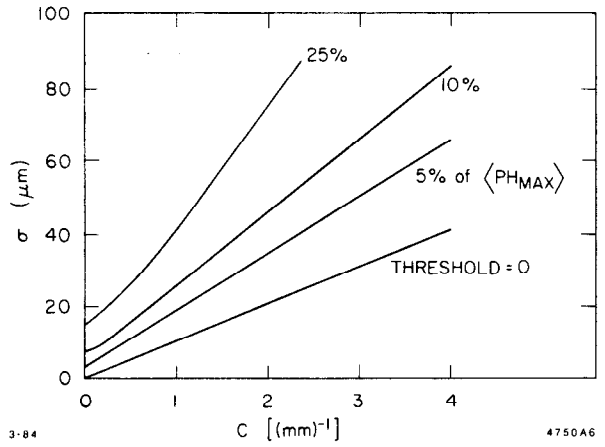

Fig. 11. Result of a Monte Carlo simulation of the resolution of a micro-jet chamber using a diffusionless gas. The different curves are for different triggering levels. The parameter C is defined in the text.

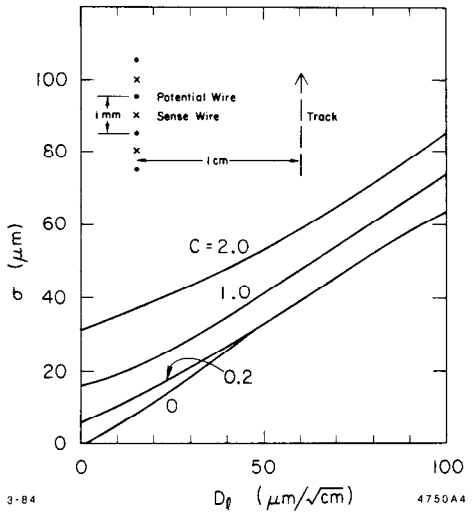

Fig. 12. Result of the Monte Carlo simulation of the resolution as a function of the diffusion constant of the gas. The inset shows the pattern of wires giving these results and those in Fig. 11.

One practical problem which arises for small cell widths compared to the length of the wires is electrostatic stability. This is illustrated in Table IV. The tension which is required to maintain electrostatic stability rises very rapidly as the cell width is reduced. The placement of additional wires (grid wires) on the cell boundary lines as shown in the insert of Fig. 13 can reduce the required tension by a large factor.

TABLE IV

Dependence of some parameters on cell width in the the jet chamber of Fig. 12. The length of the wires is 50 cm and gravitational sag is not included.

cell width (mm)	7	3	1	.5
Tension (grams)	.20	6.1	83	380
C (cm^{-1})	1.1	1.7	4.5	9.8
Cell efficiency	1.0	1.0	.95	.23
$X = Q_{pot}/Q_{sense}$	-.26	-.68	-.89	-.94

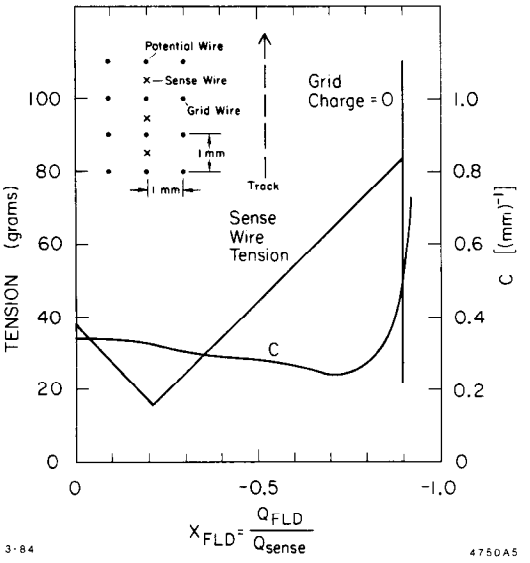

Fig. 13. The addition of a grid of wires as shown in the inset of this figure provides a free parameter x which can be varied while keeping the drift field and gain constant. This graph shows how the sense wire tension required for electro-static stability and the parameter C depend on x.

The voltage on the grid wires can be set independently with respect to the sense wire and potential wire voltages. This introduces a degree of freedom. Let the free parameter be the ratio of the potential wire charge to the sense wire charge and call it x. Then as x is varied the operating point (gain and drift field values) can be kept constant.

When this is done, the wire tension for electrostatic stability has a minimum value at a certain value of x (Fig. 13) and the value of C near this minimum of tension is smaller than it was without the grid wires. Thus the addition of the grid wires makes the smaller cell size practical by reducing the required wire tension.

At this time testing of a prototype chamber with this arrangement of wires has begun. The prototype has the following parameters: cell width = 1.5 mm; sense wire diameter = 20 μm; potential and grid wire diameter = 76 μm; grid wire to potential wire distance = 1.5 mm.

Considerable care is exercised in keeping the wire spacing uniform. The rms deviation of the wire position form its correct position has been measured as 2 μm. This is accomplished by winding the wires on a frame with very precisely machined grooved edges. The grid of wires on the frame is then transferred and glued to the chamber structure. It is necessary to make corrections as the glue sets and this is done by making measurements with a traveling microscope during the cure period.

ACKNOWLEDGEMENTS

I have gathered information from several sources. I appreciate talks from several sources. I appreciate talks with J. A. Jaros, K. G. Hayes, D. M. Ritson at SLAC, J. Va'vra at CERN and W. T. Ford at the University of Colorado. H. O. Ogren of Indiana University made important contributions to the development of the mylar tube chamber.

REFERENCES

1. John A. Jaros, "The MARK II Secondary Vertex Detector," in Proceedings of the International Conference on Instrumentation for Colliding Beam Physic, SLAC-Report 250, June 1982.
2. J. A. Jaros et al., Phys. Rev. Lett. 51, 955 (1983).
3. N. S. Lockyer et al., Phys. Rev. Lett. 51, 1316 (1983).
4. J. M. Yelton et al., SLAC-PUB-3274, Feb. 1984.
5. U. Becker et al., Nucl. Instrum. Methods 180, 61 (1981).
6. Precision Paper Tube Co., Wheeling, Illinois.
7. Emerson and Cuming Eccobond 66C.
8. A. N. Chilingarov, private communication.
9. G. B. Chadwick and F. Muller, MAC NOTE 683, unpublished.
10. J. Va'vra, SLAC-PUB-3131, June 1983.
11. E. R. Belau et al., Nucl. Instrum. Methods 192, 217 (1982).
12. J. Va'vra, Nucl. Instrum. Methods 217, 322 (1983).
13. J. Heintze, Nucl. Instrum. Methods 196, 293 (1982).